Extended Abstracts of the 22nd (1990 International) Conference on Solid State Devices and Materials, Sendai, 1990, pp. 365-368

A Band-to-Band Tunneling MOSFET Using a Thin Film Transistor

H. S. Momose, S. Kambayashi, H. Kawaguchi, I. Mizushima, S. Onga, and J. Matsunaga

ULSI Research Center, Toshiba Corporation
1, Komukai-Toshiba-cho, Saiwai-ku, Kawasaki, 210, Japan, Fax: 44-549-2267

The band-to-band tunneling phenomenon was utilized in a thin poly Si film transistor operation. It was found that the band-to-band thin poly Si film transistor has advantages over the normal operation thin poly Si film transistor, regarding gate length dependence and operating temperature dependence.

INTRODUCTION

As MOSFETs have become smaller, the band-to-band tunneling phenomenon, caused by gate-to-drain electric field, has become significant, and many studies on this phenomenon have been reported [1-4]. A new transistor mode has been proposed, which makes use of this effect, in which the drain-to-substrate band-to-band tunneling current is controlled by the gate bias [5,6]. In the experiment, a poly Si film, crystalized from an amorphous silicon film, was used as the thin film. In this paper, band-to-band tunneling is utilized in a thin film transistor and $(BT)^2$TFT (Band-To-Band Tunneling Thin Film Transistor) operation is reported for the first time.

EXPERIMENTS AND RESULTS

Figure 1 (a) shows a cross-section through the $(BT)^2$TFT used in this experiment and the bias conditions adopted. The cross-sections and the bias conditions for a band-to-band tunneling bulk transistor ($(BT)^3$) and normal operation TFT are also shown in Figs.1 (b) and (c), respectively. Device parameters for the transistors are listed in Table 1. In the experiment, a poly Si film, crystalized from an amorphous silicon film, was used as the thin film. First, the amorphous silicon film was deposited by SiH_4 LPCVD at 550°C. Then, the film was crystalized by 10 hour annealing in a nitrogen atmosphere at 600°C. The crystal size was around 0.5 μm.

Figures 2(a) and 2(b) show the I_D-V_D characteristics for $(BT)^2$TFT and $(BT)^3$, respectively. Figures 3(a) and 3(b) show subthreshold I_D-V_G characteristics for $(BT)^2$TFT and the $(BT)^3$, respectively. Almost identical characteristics were obtained, although the current magnitudes differed between the $(BT)^2$TFT and the $(BT)^3$ cases, because the gate oxide thicknesses were different. Leakage current at high drain and low gate biases for $(BT)^2$TFT are normal channel current between the source and drain. This leakage current is turned-on by the higher gate voltage, with respect to the p thin-film-substrate potential, which is determined by the drain bias via the forward drain-substrate junction. In this experiment, the n^+ region was used as the drain, because there was no p thin-film-substrate contact. However, if p thin-film-substrate was used as the drain, as in the $(BT)^3$ case, no leakage current would be observed.

In this experiment, the gate oxide thickness for $(BT)^2$TFT was much thicker than that for $(BT)^3$. The $(BT)^3$ current drive I_D and S factor dependences on the gate oxide thickness were measured. The results are shown in Fig.4. The figures show that the $(BT)^2$TFT I_D and S factor are on the gate oxide thickness dependence lines for $(BT)^3$. Thus, if the $(BT)^2$TFT gate oxide thickness is reduced to that for $(BT)^3$, characteristics similar to those for $(BT)^3$, as shown in Figs. 4(a) and 4(b), will be obtained.

Figure 5 shows the I_D-V_G characteristic short channel effects for the $(BT)^2$TFT and the normal operation TFT. The short channel effect for the $(BT)^2$TFT is very small, because the tunneling phenomenon occurs locally, and thus I_D for the $(BT)^2$TFT is inherently independent from the channel length.

Figure 6 shows I_D dependence on operating temperature. The $(BT)^2$TFT temperature dependence was smaller than that for the normal operation TFT. Basically, the tunnel current has very small temperature dependence. Probably, the $(BT)^2$TFT temperature dependence is caused by indirect tunneling via some intermediate states [3].

Figure 7 (a) shows the $(BT)^2$TFT cross-section view. The $(BT)^2$TFT size is smaller than the normal operation TFT (Fig.7 (b)), because p thin-film-substrate can be used as the drain. In addition, a $(BT)^2$TFT current dependence on the gate length and the operation temperature are better than those for a normal operation TFT. This is because that the $(BT)^2$TFT structure requires only one n-p reverse biased junction and controlled gate on it.

CONCLUSION

Band-to-band tunneling transistor operation was observed in a thin film transistor structure. It was found that the band-to-band thin film transistor ($(BT)^2$TFT) has advantages over the normal operation thin film transistor, regarding gate length and operating temperature dependences, as well as in regard to its small size. Thus, it has a potential to built very small and low current device.

ACKNOWLEDGEMENT

The authors would like to thank M. Kashiwagi and K. Natori for their continuous encouragement during the work.

REFERENCES

[1] C. Chang and J. Lien, "Corner-field induced drain leakage in thin oxide MOSFETs," *IEDM Tech. Dig.* pp.714-717, December, 1987.

[2] T. Y. Chan, J. Chen, P. K. Ko and C. Hu, "The impact of gate-induced drain leakage current on MOSFET scaling," *IEDM Tech. Dig.*, pp.718-721, 1987.

[3] H. Sasaki, M. Saitoh and K. Hashimoto, "Hot-carrier induced drain leakage current in n-channel MOSFET," *IEDM Tech. Dig.*, pp.726-729, 1987.

[4] R. Shirota, T. Endoh, M. Momodomi, R. Nakayama, S. Inoue, R. Kirisawa and F. Masuoka, "An accurate model of subbreakdown due to band-to-band tunneling and its application," *IEDM Tech. Dig.*, pp.26-29, 1988.

[5] E. Takeda, H. Matsuoka, Y. Igura and S. Asai, "A band-to-band tunneling MOS device (B^2T-MOSFET) --A kind of S_i quantum device --," *IEDM Tech. Dig.*, pp.402-405, 1988.

[6] K. Nagai , T. Tsuchiya, T. Kishi and Y. Hayashi, "I-V characteristics of a drain inversion layer," *Extended Abstracts, the 37th Spring Meeting, JSAP,* p.571, 1990.

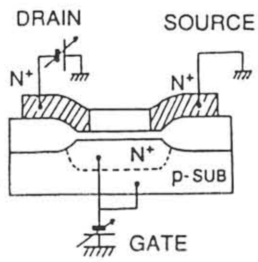

(a)

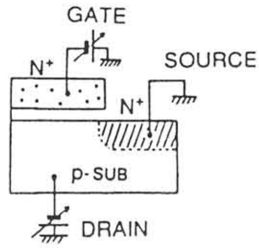

(b)

Table 1. Transistor device parameters.

THIN FILM TRANSISTOR	T_{OX}=40nm T_{POLY}=41nm W/L=0.8μm/4.0μm C_B: NO DOPING
BULK TRANSISTOR	T_{OX}=6–25nm W/L=10μm/10μm C_B=1x10^{17}cm^{-3}

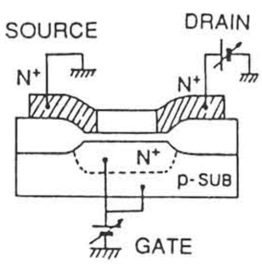

(c)

Fig 1. Transistor cross-section and bias conditions.

(a) Band-to-band thin film transistor: $(BT)^2$TFT

(b) Band-to-band bulk transistor: $(BT)^3$

(c) Normal operation thin film transistor

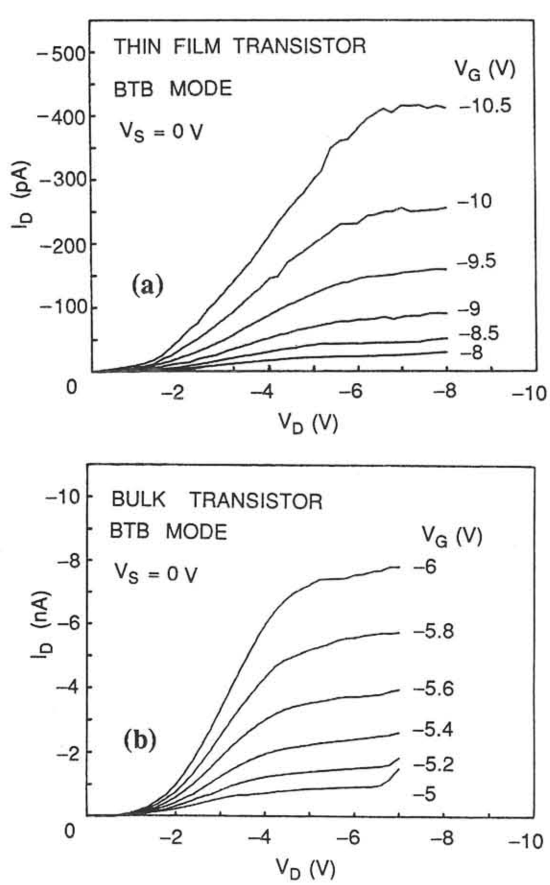

Fig 2. I - V characteristics for transistors

(a) I_D - V_D for $(BT)^2$TFT

(b) I_D - V_D for $(BT)^3$

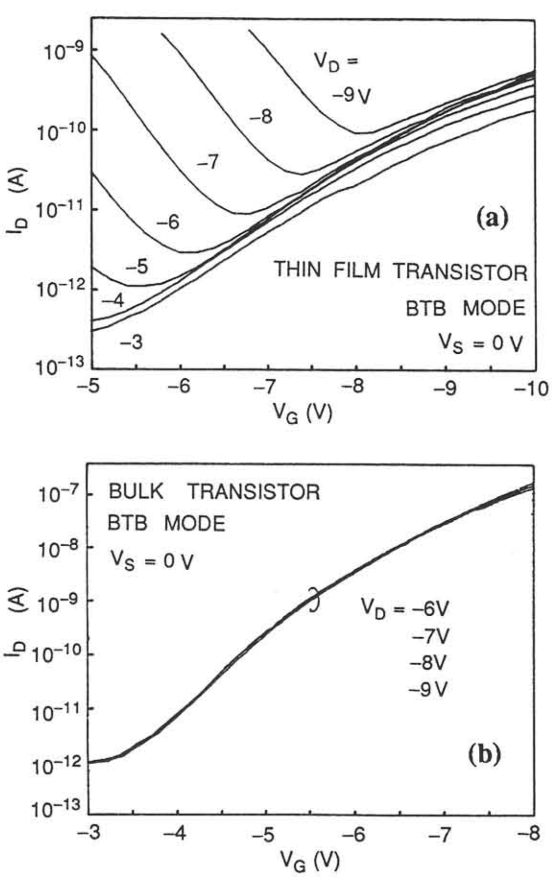

Fig 3. I - V characteristics for transistors

(a) I_D - V_G for $(BT)^2$TFT

(b) I_D - V_G for $(BT)^3$

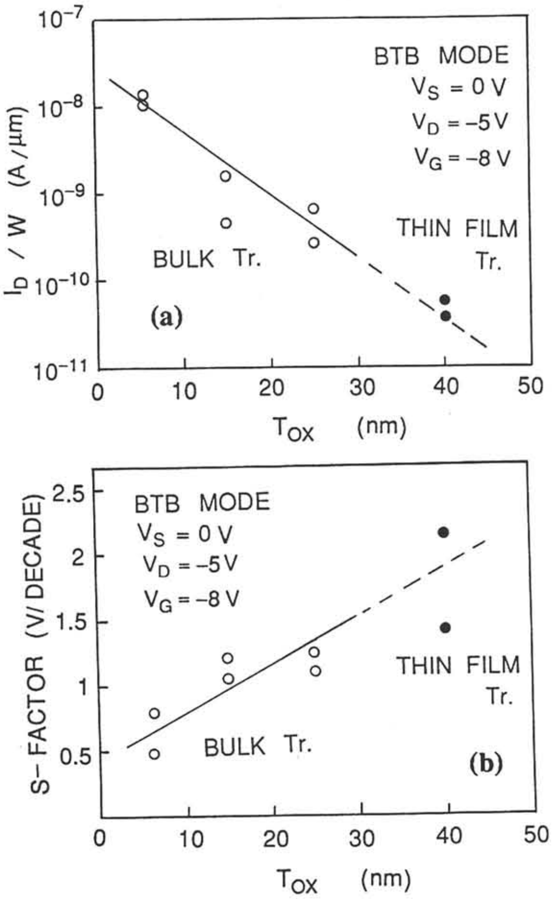

Fig 4. Gate oxide thickness dependence of $(BT)^2$TFT and $(BT)^3$ on
(a) Current drive I_D
(b) Subthreshold slope S factor

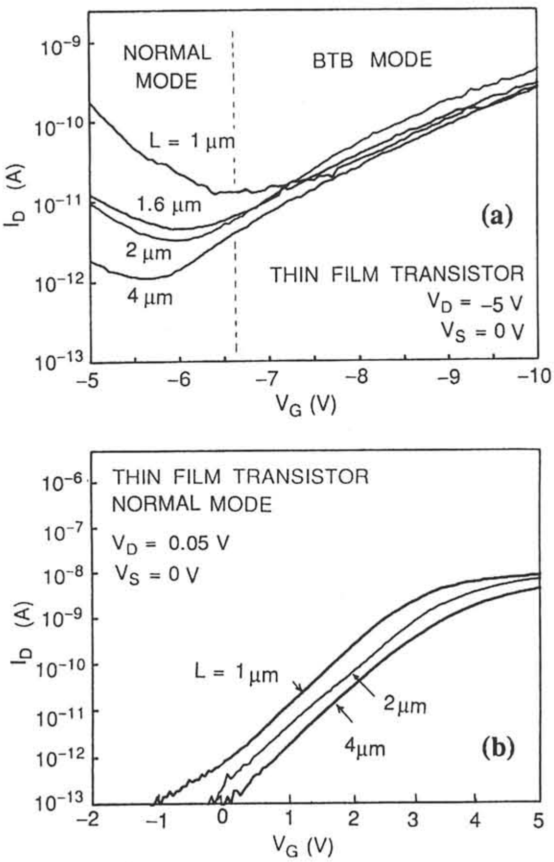

Fig 5. I_D - V_G dependence on gate length.
(a) $(BT)^2$TFT
(b) Normal operation TFT

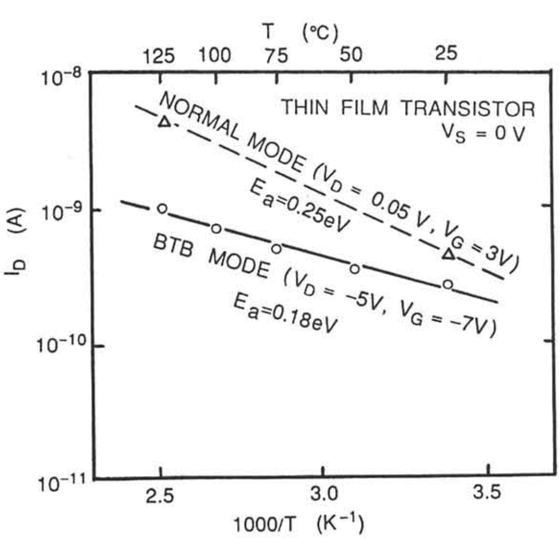

Fig 6. I_D dependence on operating temperature

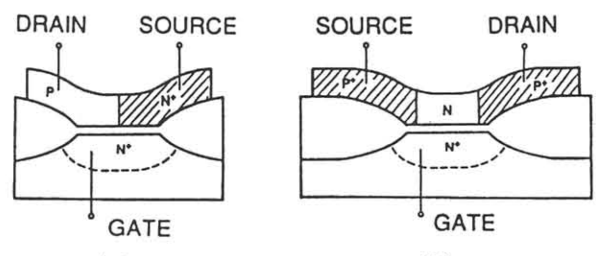

Fig 7. Transistor cross-sections
(a) $(BT)^2$TFT cross-section view
(b) Normal operation TFT cross-section view